JOURNAL OF CATALYSIS **168,** 321–327 (1997)
ARTICLE NO. CA971649

Fluorination of USY and Modification of Its Catalytic Properties

Alexander G. Panov, Vladimir Gruver, and Jose J. Fripiat[1]

Department of Chemistry and Laboratory for Surface Studies, University of Wisconsin-Milwaukee, Milwaukee, Wisconsin 53211

Received June 26, 1996; revised January 23, 1997; accepted February 5, 1997

A set of ultrastable Y zeolites with different amounts of framework and nonframework aluminum was prepared by fluorination of H-USY zeolite. The samples were characterized by chemical analysis, physical adsorption of nitrogen at low temperature and of pentane at room temperature, XRD, ^{29}Si, and ^{27}Al MAS NMR. *n*-Pentane isomerization has been studied mainly at 285°C, while the activation energy was measured on several samples. The fluorine treatment removed Al from the framework position and stabilized the zeolite structure. Hence, it decreases the number of Brønsted sites. Despite an increase in the amount of nonframework aluminum, the number of Lewis sites decreases; this means that the dispersion of the Lewis sites on the nonframework alumina particles decreases dramatically. The catalytic activity appears to be a direct function of both the number of Lewis and the number of Brønsted acid sites. These numbers being close to one another, it might be that the "acid site" is, in fact, a complex resulting from the interaction between the proton donor and an electron acceptor.

INTRODUCTION

It was reported in the literature that the fluorination of zeolites can increase its catalytic activity in acid catalyzed reactions. Different fluorination treatments were proposed (Table 1). Lok *et al.* treated different zeolites with F_2 gas and reported structural dealumination and stabilization and, in some cases, observed an increase in the catalytic activity in *n*-butane cracking (1). Aneke *et al.* added aluminum fluoride to H-Y zeolite as a promoter (2). Penchev *et al.* modified CaY zeolite with aqueous HF (3). Becker and Kowalak observed a considerable increase in catalytic activity in cumene cracking of mordenites and faujasites treated with NH_4F (4, 5) and CH_3F (4). An increase in catalytic activity in pentane isomerization on fluorinated mordenites was observed by Bursian *et al.* (6).

One result of fluorination is the zeolites' dealumination (1, 4). It has been reported that dealumination may increase the catalytic activity in the reactions catalyzed by acid sites (7–10). Sohn *et al.* assigned the increase in activity of Y zeolites, dealuminated by treatment with $SiCl_4$, in hexane cracking to an increase in the concentration of the strong Brønsted sites associated with the Al atoms with no next nearest Al neighbor in the 4-rings. In the case of mordenites fluorinated with NH_4F or CH_3F (5, 11), an increase in the acid strength was shown by calorimetric measurements of the heat of NH_3 adsorption. Ghosh and Kydd found an increase in the strength of Lewis acid sites of H-mordenites treated with HF aqueous solutions (12). Bursian *et al.* found that the number of strong Lewis sites goes through a maximum with increase in fluorine content for mordenites that were treated with HF (6).

It seems that there is an optimum F content for maximum catalytic activity; the optimum content seems to be about 1% F w/w. However, the characterization of the catalysts given in the literature has not been detailed enough to evidence which factor is implied in the modification of the catalytic activity of fluorinated zeolites.

There is a general consensus that fluorination provokes dealumination of the lattice, irrespective of the fluorination agent. Hence, the expected result of the dealumination is a decrease in the number of Brønsted sites while the number of strong Brønsted sites increases relative to the number of aluminum because of an increase in the number of isolated Al. The number of Lewis sites might increase because of the increase in the nonframework aluminum content.

Thus, the maximum observed in the variation of the catalytic activity with F content could result from the interplay of these three factors. Since no documented observation had been proposed so far, the present contribution was carried on to understand the nature of the modifications brought about by fluorine in a quantitative manner and to relate them to the catalytic activity of the modified zeolite with respect to a model reaction, namely, the transformation of *n*-pentane. The USY zeolite was chosen for this work because it already contained relatively large amounts of nonframework Al which is able to react with fluorine. Indeed, Becker and Kowalak suggested that a considerable increase in the catalytic activity and acidity of the fluorinated zeolites could be due to an interaction of Al-F species formed in the intracrystalline space with existing protonic sites (4, 11).

Different techniques developed earlier in the laboratory to characterize the acidity will be applied. It will be shown

[1] To whom correspondence should be addressed.

0021-9517/97 $25.00

TABLE 1

Summary of the Literature Data

Zeolite	Treatment	F, % w/w	Characterization	Reaction	Catalytic activity
H-Zeolon[1]	F_2 gas	n.a.	XRD, IR, crystallinity preserved; dealumination and structural stabilization	*n*-Butane cracking	Decreases in case of severe treatment; increases in case of milder treatment
NH_4Y[1]	F_2 gas	n.a.	XRD, IR. crystallinity preserved; dealumination and structural stabilization	*n*-Butane cracking	As above
H-Mordenite[6]	HF aqueous solutions	0–4	IR, CO adsorption. Decrease in the number of Brønsted sites; intensity of CO band at 2225 cm^{-1} (CO adsorbed on strong Lewis sites) goes trough a maximum with increase in F content	Pentane isomerization	Maximum activity observed for F content ~1.5% w/w
H-Mordenite[12]	HF aqueous solutions	~0.4	IR of adsorbed Pyridine. Increase in the number of strong Lewis sites. For severely treated samples the number of Brønsted and Lewis acid sites decrease	Cumene cracking (400°C)	Decreases for severely treated samples
H-Mordenite, H-ZSM-5[4]	NH_4F aqueous solutions	0–1.2	IR, XRD, NH_3 microcalorimetry. Dealumination; decrease in the number of Brønsted sites; increase in the strength of acid sites	Cumene cracking	Maximum in activity observed. The F concentration at the maximum activity is a function of Al content of the starting zeolite
AlY[4]	NH_4F aqueous solutions	0–2.5	IR, XRD, NH_3 microcalorimetry. Dealumination; increase in the population of stronger acid sites	Cumene cracking	Maximum in activity for F content ~1.5%
AlY[4]	CHF_3	0–2	As above	Cumene cracking	Maximum in activity for F content ~0.5%

that fluorination of USY results in a loss of activity due to a decrease in the number of Brønsted sites which is not compensated by an increase in Lewis acidity.

EXPERIMENTAL

Material

The parent USY zeolite is a commercial PQ product with a Si/FAl ratio of 4.9, determined by NMR (FAl, framework aluminum). The fluorinated samples were prepared by impregnating the original USY zeolite with 3–5 mL of the NH_4F solution per gram of zeolite. In order to control the fluorine content in the solid, the amount of NH_4F in the solutions used for impregnation was varied. The total F content in the solutions was either 1.5, 3, 5, 7.5, and/or 10% w/w, with respect to the amount of zeolite used. Almost all fluorine was adsorbed by the zeolites during impregnation, fluorine being not detectable in the solutions. After impregnation the samples were dried at 60°C and calcined in the oven at 250 and 550°C overnight. We shall refer to the samples as USYF1.5, USYF3, USYF5, USYF7.5, and USYF10. The final F contents were between 1 and 2.1 as shown in Table 2. The sample USY500 is a commercial USY, USY550 is the starting zeolite calcined at 550°C, and USY500* is USY500 pretreated in a flow of oxygen, namely the standard treatment before catalytic testing (see below).

Material Characterization

The chemical analysis for fluorine was performed using the colorimetric zirconium eriochrom cyanine R method (13). The fluorine concentration in the solutions which had been used for impregnation was determined as well.

The Si/FAl (aluminum) ratio was obtained from ^{29}Si NMR. The Si and Al total contents for USY500 were from the chemical analysis. The Si/Al_{tot} ratios for selected samples were also measured using an EDX system attached to SEM. The data are presented in Table 2. The Si/Al_{tot} ratios measured by EDX were close (±6%) to that of USY500, so we assumed the value of $Si/Al_{tot} = 2.6$ for all fluorinated samples. From Si/FAl and Si/Al_{tot} ratios assuming that Si is not dislodged from framework position and that the catalysts consist mainly of zeolites (actually it was ≥90%), the number of framework (FAl) and nonframework aluminum (NFAl) are easily calculated (Table 2). From Si/FAl the

TABLE 2

Physical Characteristics and Fluorine Content of the Fluorinated USY

Sample	F before calcination, wt%	F after calcination, wt%	Surface area, m^2/g	Surface area of macro- & mesopore m^2/g	Micropore volume, ml/g	Langmuir volume, pentane, ml/g	Crystallinity, %	u.c. parameter (Å)
USY500	0	0	803	18.5	0.287	0.219	100	24.52
USY550	0	0	858	52.3	0.279	0.230	92.3	24.44
USY1.5F	1.5	1	783	50.54	0.257	0.223	101.4	24.54
USY3F	3.0	1.1	804	53.4	0.263	0.207	114.6	24.47
USY5F	4.0	1.6	767	43.1	0.254	0.198	106.5	24.47
USY7.5F	6.6	1.5	711	38.7	0.237	0.171	116.3	24.44
USY10F	9.1	2	649	50.3	0.208	0.167	122.1	24.37

number of Brønsted sites made from an OH bridging silicon to aluminum in the cluster $^4Q(1Al)$ can be calculated, as well as the number of strong Brønsted sites FAl_1, where aluminum has no next-nearest Al neighbor (14). In compliance with the nomenclature that we have used before, the former Brønsted sites are called Q_1, while the latter are called FAl_1. Q_1 results from a empirical equation obtained from a Monte-Carlo simulation

$$Q_1/Si = (FAl/Si)(1 - FAl/Si)^3, \quad [1]$$

whereas

$$FAl_1/(FAl + Si) = \alpha(1 - \alpha)^\beta, \quad [2]$$

where $\alpha = FAl/(FAl + Si)$. β is 9 for Y zeolites; it corresponds to the total number of next neighbor sites to an aluminum (14).

N_2 and pentane adsorption–desorption isotherms were measured at liquid nitrogen and room temperature (298 K), respectively. The specific surface areas shown in Table 2 are the Langmuir surface areas, calculated from a Langmuir plot in the domain $p/p_o = 0.01$–0.4. The surface areas of the macro- and mesopores, and the microporous volume were calculated using the *t*-plot algorithm. The ratio of the Langmuir volume measured by pentane adsorption to the theoretical micropore volume of Y zeolite (0.33 mL/g) (V_{av} in Table 3) was used as an availability index of the zeolite lattice to pentane (15).

The XRD spectra were obtained using a Scintag X-ray, $\Theta - \Theta$, diffractometer: Cu$K\alpha$ radiation and a scan rate of 5°/min at room temperature. A NBS standard silicon was used to calibrate the diffraction angle, and, in all cases, the 2Θ value of Si(111) was within $\pm 0.01°$ from the theoretical value (28.443°). The 2Θ positions of the 111, 220, 311, 511, 440, 533, and 642 reflections were used to calculate the average unit cell parameter. The areas of 220, 311, 331, 511, 440, 533, and 642 reflections were used to calculate the degree of crystallinity (15). The crystallinity of USY500 was taken as reference and considered as 100%.

The catalytic activity in pentane isomerization was measured at 285°C in a flow stainless steel reactor using H_2 as a carrier and pentane: hydrogen ratio = 1 : 2; WHSV 4–16 h; and 3 atm total pressure. The products were analyzed with an on-line GC. Linear variation between conversion and contact time were obtained. The catalytic activity (pentane molecules transformed per minute per gram of catalyst) is

$$a = \frac{1}{60}\frac{dX}{d\tau}\frac{N_a}{M}, \quad [3]$$

where X is the conversion, τ is the contact time (1/WHSV), N_a is the Avogadro number, and M is the pentane molecular weight. The activation energies for the selected samples were measured with a recirculation catalytic system at atmospheric pressure with a pentane pressure of 50 torr and an H_2 pressure of 700 torr. Before use, the catalysts were pretreated in a flow of oxygen. The temperature was increased at the rate of 2°C/min and kept constant for 2 h at 150, 300, and 450°C.

TABLE 3

Chemical Characterization of the Fluorinated USY Samples

Sample	Si/Al (a)	Si/FAl (b)	FAl/u.c. (c)	NFAl/g. $\times 10^{-20}$ (d)	Q1/g. $\times 10^{-20}$ (e)	Al_1/g $\times 10^{-20}$ (f)	Aval., % (g)
USY500	2.6	4.9	32.54	9.32	9.03	3.2	0.60
USY500*	2.6	5.9	29.09	11.05	8.61	3.5	0.60
USY550	2.6	6.9	24.40	13.50	7.91	3.7	0.60
USY1.5F	2.4	6.6	25.26	13.39	8.05	3.7	0.58
USY3F	2.6	12.1	14.66	18.97	5.80	3.6	0.53
USY5F	2.7	14.0	12.80	19.00	5.27	3.6	0.52
USY7.5F	2.6	18.7	9.75	21.92	4.30	2.4	0.44
USY10F	2.6	59.4	3.18	26.07	1.64	1.4	0.42

Note. (a) Si/Al molar ratio obtained from chemical analysis; (b) Si/framework Al ratios obtained from ^{29}Si NMR; (c) framework Al per unit cell; (d) nonframework Al per g; (e) theoretical number of Brønsted sites per gram; (f) theoretical number of aluminum with no next-nearest aluminum neighbors, or strong Brønsted sites; (g) ratio of the micropore volume available to *n*-pentane to the theoretical pore volume (see Fig. 1).

TABLE 4

Isomerization and Cracking Activity at 285°C

Sample	Isom. cat. act, molec./min./g $\times 10^{-18}$	Crack cat. act. molec./min./g $\times 10^{-18}$	Activation energy, isomer., kcal/mol	Lewis sites/g $\times 10^{-20}$	Brønsted sites (total)/g $\times 10^{-20}$
USY500*	41.9	7.0	18 ± 1	8.6	8.5
USY550	32.1	4.1	—	5.9	4.8
USY1.5F	33.5	4.2	19 ± 2	6.0	5.0
USY3F	19.5	2.8	19.4 ± 0.2	5.3	2.5
USY5F	22.3	2.8	—	4.7	3.7
USY7.5F	11.2	1.4	—	5.4	1.9
USY10F	2.8	—	18 ± 2	2.0	1.4

Note: Activation energy of the isomerization reaction. Number of Brønsted and Lewis acid sites derived from ammonia adsorption.

Acidity Measurements

Because some of the concepts at the origin of the acidity measurements performed on these samples are rather new, the significance of the acidity data will be explained. First, an infrared study of low temperature CO chemisorption had shown a doubling of the CO stretch assigned to the interaction with acidic OH in USYnF (n = % content in fluorine). The high frequency component observed at 2177 cm^{-1} in USYnF has been assigned to CO interacting with the strongly acidic OH, or FAl_1. However, the CO band with a maximum at ~2168 cm^{-1} cannot be assigned unambiguously. Moreover, in USYnF, the Lewis acidity, if any, was not indicated by spectral features between 2190 and 2230 cm^{-1} in the CO spectrum, as had been observed in dealuminated mordenite or in dealuminated ZSM-5 (16–19).

In the chemisorbed ammonia FTIR spectra the strong Brønsted sites correspond to a band with maximum near 1400 cm^{-1}, whereas the weaker ones contribute to the band with maximum near 1450 cm^{-1} (20). The Lewis sites are characterized by two bands, one with maximum near 1625 cm^{-1} and the second one with a frequency between 1300 and 1330 cm^{-1}.

The negative aspect of using CO as a probe for quantifying the number of sites is the large discrepancy between published extinction coefficients. For these reasons, and as shown elsewhere (20), NH_3 has been preferred. Extinction coefficients for $L:NH_3$ or NH_4^+ bands at 1625 and ~1450 cm^{-1}, respectively, are known (21) and the resolution of the infrared spectrum in bands attributable to Lewis and Brønsted sites is obtained after outgassing at different temperatures between 115° and 350°C.

The amounts of strong Brønsted sites obtained from the ammonia FTIR-TPD study are in Table 4, as well as the amount of Lewis sites, the latter being defined empirically as the number of ammonia molecules remaining adsorbed after outgassing 30 min at 115°C (20). The reason for this choice is supported by the agreement between the intensity of the ^1H NMR resonance line of NH_3 on Lewis sites with the integrated intensity of the NH_3 bending IR vibration at 1625 cm^{-1}, as shown in Ref. (20).

RESULTS

The results of chemical analysis for F, Si/Al_{tot}, the Si/Al NMR ratio, the framework and nonframework Al contents are presented in Tables 3 and 4. After calcination most of the fluorine was removed and the final F contents were in the 1–2% range. These results are close to those reported by Becker and Kowalak for aluminated Y zeolites, fluorinated in about the same way (4). The content of FAl decreased sharply with an increase in fluorine concentration (Fig. 1A). The ^{29}Si NMR spectra of samples which were not calcined at high temperature showed that the dealumination took place during the calcination at 550°C. The micropore volumes available to N_2 and pentane decreases with increasing NFAl content (Fig. 1B).

XRD diffraction showed that the fluorinated USY kept its crystallinity. It even increased as the number of framework Al decreased. The crystallinity of the USY calcined at 550° decreased slightly (Table 2). Formation of an amorphous phase was not observed. However, for the samples USY7.5 and USY10 two very weak diffraction lines appear at 2Θ 14.5° and 16.35°, indicating the crystallization of minute amounts of AlF_xO_y probably outside the zeolite particles.

The lattice parameter, calculated from 2Θ positions of the diffraction lines by using a simulation program built into the Scintag software decreased from 24.6 Å (for 30 Al per uc) to 24.3 Å (for 3 Al per uc). The decrease in

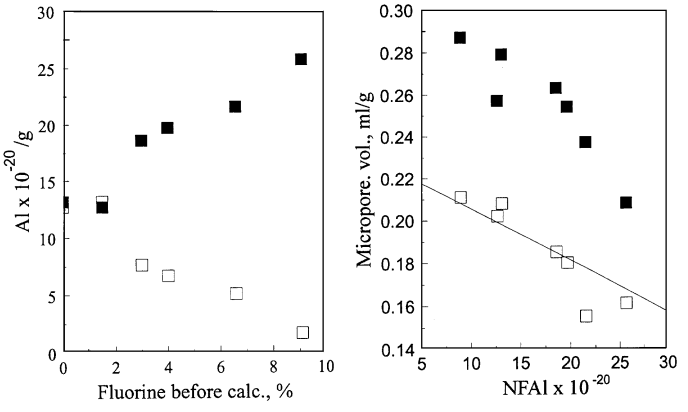

FIG. 1. (A) Increase (■) of nonframework aluminum content (NFAl) and decrease (□) of the framework aluminum content (FAl) as a function of the amount (wt%) of NH_4F used to impregnate USY prior to calcination. (B) Decrease of the micropore volume available to N_2 (■) or to a *n*-pentane (□) as a function of the amount of NFAl. The straight line represents the theoretical variations calculated by Yong *et al.* (14).

the unit cell parameter is indicative of zeolite lattice dealumination. Several linear relationships between the unit cell (uc) dimension and the number of Al per uc were proposed in the literature (22–24). The correlation between unit cell parameter and FAl content for the samples obtained by calcination (USY500 and USY550) fits well the equation proposed by Kerr; see Ref. (23). For the fluorinated samples, the FAl content per uc obtained from ^{29}Si NMR fit into a linear regression which is shifted from that fitting USY500 and 550 (Fig. 2), suggesting that fluorination does not result only in dealumination, but that it also leads to structural stabilization and probably reconstruction of the zeolite structure. An attempt was made to locate fluorine with respect to Si or Al by NMR spectroscopy in J. F. Haw's laboratory (25). The existence of Si-F linkage appears to be ruled out because no polarization transfer ^{19}F-^{29}Si was observed in the calcined samples. Probably, fluorine is linked to Al, as suggested by the weak X-ray diffraction lines observed at high fluorine content. Before calcination the nature of the absorption site for fluorine was unknown.

As suggested by Lok *et al.* (1) dealumination obtained upon fluorination results primarily at the opening of the Al–O–Si bonds by HF, followed by the expulsion of alumina moieties and reconstruction of the silicon network (1). The alumina moieties gather in the zeolite pores and form small particles which reconstruct by eventual elimination of HF and/or OH. In the absence of fluorine, the removal of surface OH in NFAl moieties is at the origin of coordinately unsaturated sites, that is, of the Lewis sites (26). In the presence of fluorine, the formation of Lewis sites may be prevented in areas rich in fluorine.

Figures 3A and B shows that a redistribution of aluminum among the three coordination states (Al^{IV}, Al^{V}, and Al^{VI}) occurs within the NFAl particles as dealumination increases. These contents were obtained using the deconvolution technique, proposed by Coster *et al.* (26) which takes into account the quadrupolar nature of the chemical shift tensor.

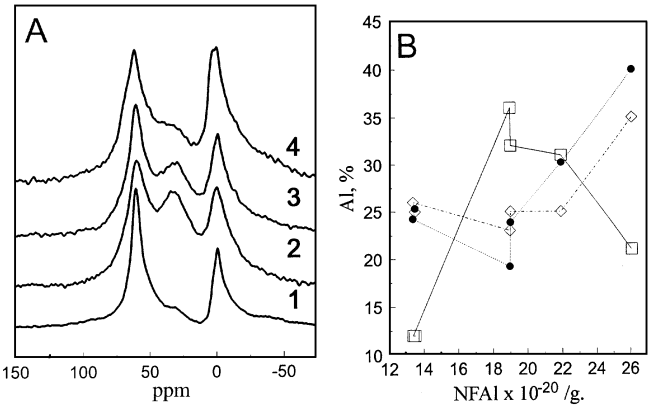

FIG. 3. (A) Selected ^{27}Al MAS NMR spectra of 1, USY550; 2, USY3F; 3, USY5F; 4, USY10F. (B) ^{21}Al MAS NMR spectra deconvolution according to the procedure suggested by Coster *et al.* (26). The Al^{IV} (◇) and Al^{VI} content (●) in the nonframework aluminum particles increase with dealumination, whereas Al^{V} (□) goes through a maximum.

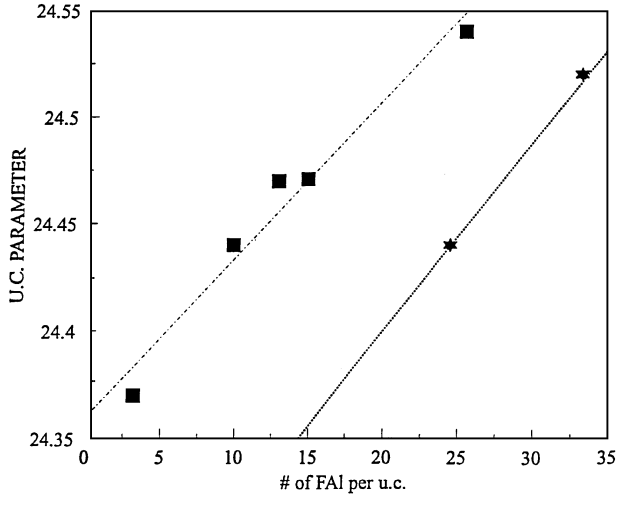

FIG. 2. Variation of the unit cell parameter (Å) with the amount of framework aluminum per unit cell: FAl/uc. The dotted line corresponds to the empirical equations suggested by Kerr (22): (■) USYnF; (★) USY500 and 550 before fluorination.

DISCUSSION

Upon calcination or steaming the number of Lewis sites in zeolites HY, HM, or HZSM-5 increases as the NFAl content increases (20). Here the situation is different since, in fluorinated USY, the number of Lewis sites decreases as the NFAl content increases.

It might be that above some concentration limit the NFAl particles begin to grow and that their surface area would decrease as suggested by Fig. 4A. Another explanation is that the lower number of Lewis sites per NFAl is due to

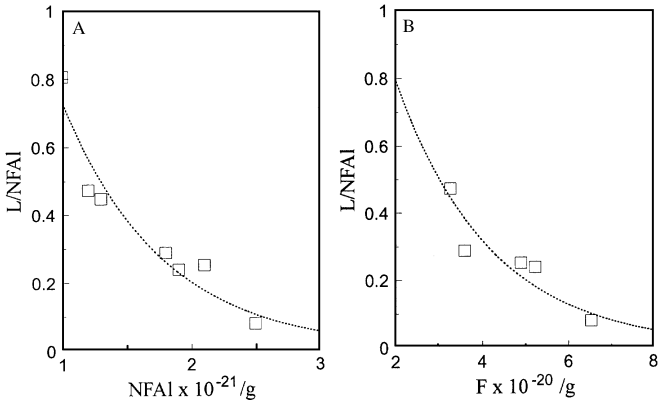

FIG. 4. (A) Variation of the ratio: number of Lewis sites per NFAl vs the NFAl content g^{-1}. (B) Decrease of this ratio vs the fluorine content after calcination.

the fact that the formation of surface uncoordinated sites is prevented by the surface fluorination. This would be the favored hypothesis suggested by Fig. 4B, since the number of Lewis sites per NFAl decreases continuously as the fluorine content increases. Of course, both the size effect and the inhibition effect of fluorine could play simultaneously.

Thus, the important consequence of fluorination is a decrease in the number of Brønsted and Lewis sites, as shown in Table 4, from the results of NH_3 chemisorption. The total number of Brønsted sites should theoretically be equal to Q_1. As shown by comparing Tables 2 and 3, Brt is lower than Q_1, the probable reason being the reaction of acid bridging OH with NFAl basic OH (27).

From the study of the acidity characteristics of USYnF, it can be predicted that the fluorinated USY is not going to be a good acid catalyst, being deficient both in Brønsted and Lewis acidity.

The isomerization and cracking catalytic activity measured at 285°C as well as the activation energy are shown in Table 4. The constancy of the activation energy, despite large differences in compositions and the quasi-constancy of the ratio of the isomerization to the cracking rate indicate that the reaction mechanism is not affected by the nature of the sample. Therefore, a comparison of the rate constants (or catalytic activity, *a* in Eq. [3]) with respect to the number and quality of acid sites is meaningful. First, and in agreement with a dealuminated Y zeolite study (DHY) by Yong *et al.* (27), USYnF is mainly an isomerization catalyst in the 300°C range. In contrast, DHZ is mainly a cracking catalyst. In order to evidence the role played by the Brønsted and/or the Lewis acid sites, we have plotted (Fig. 5) the experimental isomerization rate with respect to the number of available acid sites.

The data in Fig. 5 suggest that both sites play a role. The simplest way to interpret this observation is by accepting the fact that a pair of Brønsted and Lewis sites constitute one catalytic active complex site.

This suggestion is like the classical view that there is a mutual enhancement of the strengths of the Brønsted and Lewis sites, due to a synergistic interaction. An additional support for this interpretation has been recently published by Makarova *et al.* (28), showing that the strength of a Brønsted site in zeolite is enhanced by low temperature absorption of BF_3.

In the case of the fluorinated USY, the pairing of the Brønsted and Lewis sites is possible, since the numbers of both kinds of sites are close and their proximity must be increased by the accumulation of NFAl in the pore system.

If a pair of Brønsted and Lewis sites is equivalent to one complex acid site, the direct proportionality relationships shown in Fig. 5 are easily understood and the linearity versus the square root (the geometrical average) of their concentration is trivial. Figure 5 indicates a trend but does not imply a specific mechanism.

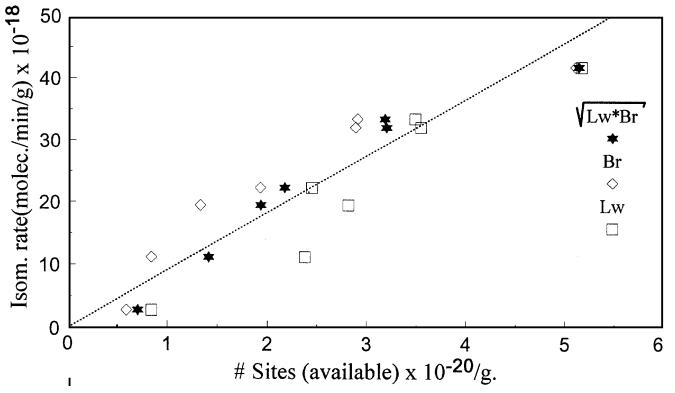

FIG. 5. Evolution of the experimental rate of isomerization vs the total number of available Brønsted sites, of available Lewis sites, and the geometric average of the numbers of Brønsted and Lewis sites. The numbers of Brønsted or Lewis sites in Table 1 are multiplied by V_{av}, Table 2.

As a first step, the isomerization on Lewis sites may involve the formation of a hydride, followed by a methyl shift.

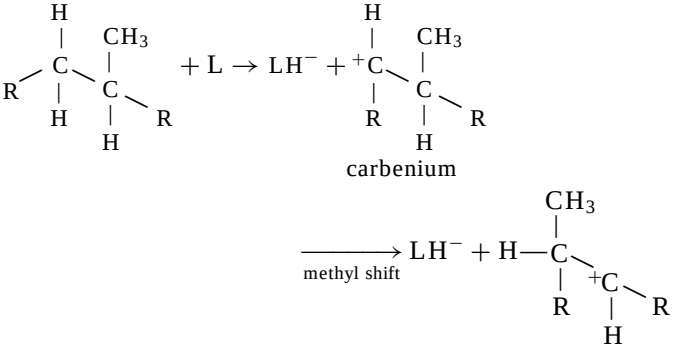

→ recombination or bimolecular hydride transfer

The enhancement of the Lewis acid strength by the Brønsted acid centers could favor this scheme. However, as recognized generally (29), there is no clear distinction between reactions catalyzed by Lewis or Brønsted sites. According to Jacobs *et al.* (30), cracking requires a stronger acidity than isomerization.

ACKNOWLEDGMENTS

This work has been made possible by DOE Grant DE-FG02 90-ER1430. Analysis of the samples was performed in the Advanced Analytical Facility of UWM (Dr. A. Sklyarov). We thank Professor J. F. Haw and his team at Texas A & M for their efforts for showing the ^{19}F and ^{29}Si or ^{27}Al interactions.

REFERENCES

1. Lok, B. M., Gorstema, F. P., Messina, C. A., Rastelli, H., and Izod, T. P. J., *ACS Synmp. Ser.* **218**, 41 (1983).
2. Aneke, L. E., Gerristen, L. A., van der Berg, P. J., and de Jong, W. A., *J. Catal.* **59**, 26 (1979).
3. Panchev, V., Sariev, I., and Zhelyazkova, M., *Kinet. Katal.* **23**, 562 (1981).

4. Becker, K. A., and Kowalak, S., *in* "Recent Advances in Zeolite Science" (J. Klinowski and P. J. Barrie, Eds.), p. 123, Elsevier, New York, 1989.
5. Becker, K. A., and Kowalak, S., *J. Chem. Soc., Faraday Trans. I* **81**, 1161 (1985).
6. Bursian, N. R., Borutsky, P. N., Georgievsky, V. Yu, Gruver, V., Krasii, B. V., Lastovkin, G. A., Martynova, G. G., Orlov, D. S., and Brovko, V. N., *Prepr. Am. Chem. Soc., Dev. Petrol. Chem.* **36**, 893 (1991); Alexandrova, N. V., Bursian, N. R., Georgievsky, V. Yu, Gruver, V. Sh., Zverev, S. M., Semenova, T. A., Semenskaya, I. V., Oranskaya, O. M., and Minachev, Kh. M., *in* "Primenenie Tseolitov Katalize," pp. 62–64, Moscow, Nauka, 1989.
7. Sohn, J. R., De Canio, S. J., Fritz, P. O., and Lunsford, J. H., *J. Phys. Chem.* **90**, 4847 (1986).
8. Shertukde, P. V., Hall, W. K., Dereppe, J. M., and Marcelin, G., *J. Catal.* **139**, 468 (1993).
9. Caravajal, R., Chu, P.-J., and Lunsford, J. H., *J. Catal.* **125**, 123 (1990).
10. Beyerlein, R. A., MacVicker, G. B., Yacullo, L. N., and Ziemiak, J. J., *J. Phys. Chem.* **92**, 1967 (1988).
11. Becker, K. A., and Kowalak, S., *J. Chem. Soc., Faraday Trans. I* **82**, 2157 (1986).
12. Ghosh, A. K., and Kydd, R. A., *J. Catal.* **103**, 399 (1987).
13. Huang, P. M., and Jackson, M. L., *Am. Minerol.* **52**, 1503 (1967).
14. Levitz, P., Blumenfeld, A. L., and Fripiat, J. J., *J. Catal. Lett.* **38**, 11 (1996).
15. Hong, Y., and Fripiat, J. J., *Microporous Mat.* **4**, 323 (1995).
16. Kustov, L. M., Kazansky, V. B., Beran, S., Kubelkova, L., and Jiru, P., *J. Phys. Chem.* **91**, 5247 (1987).
17. Bates, S., and Dwyer, J., *J. Phys. Chem.* **97**, 5897 (1993).
18. Gruver, V., Panov, A., and Fripiat, J. J., *Langmuir* **12**, 2505 (1996).
19. Gruver, V., and Fripiat, J. J., *J. Phys. Chem.* **98**, 8549 (1994).
20. Yin, Fei, Gruver, V., Blumenfeld, A. L., and Fripiat, J. J., *J. Phys. Chem. B* **101**, 1824 (1997).
21. Datka, J., Gil, B., and Kubacka, A., *Zeolites* **15**, 501 (1995).
22. Breck, D. W., and Flanigen, E. M., "Molecular Sieves," Soc. Chem. Indus. London, 1968.
23. Kerr, G. T., *Zeolites* **9**, 350 (1989).
24. Sohn, J. R., De Canio, S. J., Lunsford, J. H., and O'Donnel, D. J., *Zeolites* **6**, 225 (1986).
25. Haw, J., Texas A & M, personal communication.
26. Coster, D., Blumenfeld, A. L., and Fripiat, J. J., *J. Phys. Chem.* **98**, 6201 (1994).
27. Yong, H., Gruver, V., and Fripiat, J. J., *J. Catal.* **161**, 766 (1996).
28. Makarova, M. A., Bates, S. P., and Dwyer, J., *J. Am. Chem. Soc.* **117**, 11309 (1995).
29. Pines, H., "The Chemistry of Catalytic Hydrocarbon Conversion," p. 305, Academic Press, New York, 1981.
30. Jacobs, P. A., *Carbonogenic Activity of Zeolite*, p. 253, Elsevier, Amsterdam, 1977.